Cost-Aware Strategies for Enhancing Energy Resilience in Microgrids via Stationary and Mobile Resources

S M Safayet Ullah[a], Farzad Ferdowsi[a], Terrence Chambers[b]

[a]*Department of Electrical & Computer Engineering, University of Louisiana at Lafayette, Lafayette, 70503, LA, USA*
[b]*Department of Mechanical Engineering, University of Louisiana at Lafayette, Lafayette, 70503, LA, USA*

Abstract

The primary goal of this research study is to enhance energy resilience with a focus on cost efficiency. To achieve this objective, two key objectives have been identified: 1) reducing unserved loads, and 2) implementing cost-effective resource allocation strategies. A high-fidelity real-time model of a solar plus storage microgrid is developed to simulate a variety of what-if scenarios. This model is based on the conceptual design of a campus microgrid facility, which is slated for commissioning at UL Lafayette in close collaboration with a local power utility. The study examines the microgrid's performance under different configurations, including both stationary battery and mobile battery storage options. To ensure the realism of the scenarios, real solar data from specific days following the occurrence of three major hurricanes in Louisiana is utilized. The analysis includes an assessment of unserved loads under various scenarios, as well as an investigation into the resilience impact of investment decisions and the planning and operation of mobile storage systems. The results indicate the proposed planning and operation will improve resilience while staying within the profitable range. The resilience is quantified and compared with other scenarios providing an insightful planning framework for decision-makers.

Keywords: Energy Resilience, Renewable Energy, Microgrid

1. Introduction

Enhancing energy resilience is essential for ensuring the sustainable provision of electricity services to customers. The increasing frequency and intensity of natural disasters, such as hurricanes, wildfires, and extreme weather events, pose significant challenges to the resilience of energy infrastructure. Microgrid formation has been a popular strategy in the literature as a means to enhance energy resilience in response to outages [1; 2; 3; 4; 5]. Microgrid formation is often suggested as a way to boost energy resilience during outages. This makes sense for a few reasons: First, microgrids mostly serve local areas, so they do not rely on long-distance power lines that may get damaged in disasters. This local focus helps keep the lights on for nearby homes and businesses. Second, because microgrids are relatively new, they are built with modern standards in mind. This means they're more likely to withstand disasters and stay running when the main grid might fail. Lastly, microgrids can provide power when the main grid cannot, ensuring that critical services stay running even during emergencies.

Power utilities and service providers are increasingly interested in investing in microgrid formation to enhance energy resilience. However, their decision-making process is complex and is influenced by two key considerations: the extent to which resilience is improved and the associated costs. These questions are challenging to answer definitively due to several factors:

Scenario Dependence: The concept of resilience varies depending on the scenario. For example, improving resilience against floods may not necessarily enhance resilience against hurricanes. Therefore, the specific resilience needs of a particular location or situation must be carefully evaluated.

Measurement Metrics: Determining how to measure resilience improvement is crucial. Various metrics for resilience have been proposed in the literature [6; 7], ranging from reliability indices [8; 9; 10] to social and economic impacts [11; 12; 13; 14]. Selecting the most appropriate metrics for a given context is essential but challenging.

Cost Considerations: Understanding how costs escalate with each percentage increase in resilience is vital. This involves evaluating the costs of implementing and maintaining microgrid systems compared to the potential benefits in terms of resilience enhancement.

The investigation into the specific cause of the power outage falls outside the scope of this study. Instead, our research focuses on quantifying energy resilience and assessing the associated costs of enhancing resilience. Different resilience metrics have been proposed recently in the literature. In [15], a quantitative metric is proposed where the full service, worst performance, speed of degradation, and speed of recovery are factored in to develop a comprehensive resilience metric. However, load priorities are not set and the cost of resilience enhancement is not discussed. Authors in [16] developed a method for optimizing network reconfiguration and mobile emergency generator (MEG) deployment in smart grids. The proposed method is optimization-based. Time domain studies and economic analysis are not provided. A different resilience metric is proposed in [17] based on the measured voltage of the main DC bus. This metric allows for real-time resilience assessment and monitoring of microgrid resilience over time. The method is specifically designed for microgrids as opposed to most of the existing methods that are more applicable to larger power systems. However, the case study which is a naval ship is more mission-oriented rather than service-driven. The amount of supplied loads is a metric used in [18] to evaluate optimum microgrid formation in a distribution feeder as a resilience enhancement strategy. Load prioritization, time domain analysis, and cost studies are not provided. A similar metric is also proposed in [19; 20] where the amount and cost of unserved loads are used to measure resilience. Improvements are made by incorporating electric vehicles and solar PV into the residential feeders. The same research gaps are also seen in these two studies.

Solar plus energy storage is the most common type of microgrid formation at both residential and utility scales [21]. In addition to stationary energy storage systems, Mobile Resources (MR) play an important role in enhancing energy resilience, particularly in the context of modern power systems facing increasing challenges from natural disasters, cyber-attacks, and other disruptions. The transportability of MRs helps a lot with uncertainties with respect to the place and scale of damages to the energy system. The concept of using MRs, such as repair trucks/crews [22], mobile generators [23], energy storage units [24], and microgrids [25], has gained attention due to their ability to provide temporary power supply and restore electricity in disaster-stricken areas efficiently.

In recent years, mobile resources have been utilized in various disaster scenarios, including hurricanes [26], wildfires [27], and winter storm [28; 29], demonstrating their effectiveness in providing reliable power supply to critical infrastructure, emergency shelters, and essential services. These resources are often deployed quickly and can be relocated as needed, making them a flexible solution for addressing immediate energy needs in disaster-affected areas. Mobile resources have been discussed in different sets of literature within the past few years to improve energy resilience. In [30], an optimization problem is solved to effectively dispatch repair crews and mobile resources; however, load priorities are not considered. Furthermore, the impact on resilience is not measured. Authors in [31], proposed a strategy to optimally dispatch MRs in a 33 bus distribution system. A similar optimization-based study is conducted in [32] on a balanced distribution feeder with non-real DER data. Although most research works in the MR area are proposed and tested for distribution systems, authors in [33] proposed a real-time strategy to dispatch MRs combined with microgrid forming. A real-time optimization problem is proposed where different MRs are incorporated including EVs, mobile generators, and mobile energy storage. To the best of our knowledge, in addition to [33], in three other research works [34; 35], the real-time dispatch of MRs is proposed. However, the proposed algorithms are not tested on any real-time simulator/processor. In [35], The real-time refers to sending resources from a pre-determined location to a target location. In none of the above-mentioned studies, the real-time operation of MR is tested. Also, it is not clear how the planning/operation algorithm is implemented into the feeder or microgrid controller making real-time decisions.

In this study, a high-fidelity real-time model of a solar plus storage microgrid is created. The microgrid load is categorized into different priorities. The microgrid's resilience is evaluated under different stationary/mobile resource allocation strategies. The estimated cost of resilience improvement can serve as a guideline for decision-makers.

The technical contributions of this study include:

- Measuring the impact of stationary and mobile resources on microgrid's resilience
- Cost-aware resource allocation along with load priorities
- Incorporating real-time operation of mobile storage systems into microgrid's controller

2. Case Study

This research utilized the microgrid facility situated at the University of Louisiana at Lafayette(UL) as the case study presented in Fig. 1. Load data is collected from a real distribution feeder for this research study. All the load data is classified into three categories: priority load 1, priority load 2, and priority load 3. Here, priority load 1 is considered the most critical load and will get the highest priority during the load serving; priority load 2 is considered a moderate critical load and will get moderate priority during the load serving; priority load 3 is considered the least critical load and will get the lowest priority during the load serving. For 24-hour power outage, the load demand for the most critical, moderate, and least critical loads is 681.762 kWh, 957.701 kWh, and 638.475 kWh, respectively. The load demand profiles for these three categories are presented in Fig. 2. This research considered 24-hour power outages for three hurricanes that hit Louisiana in the past five years. Those hurricanes are Laura (2020), Zeta (2020), and Ida (2021). For these three hurricanes, power outages for 24 hours are considered where the microgrid is solely responsible for satisfying the load demands. The solar radiation data corresponding to every hurricane-affected day is collected from the University of Louisiana at Lafayette's 1.1 MW solar PV plant facility [36] to integrate more realistic approaches. The solar radiation profile for each hurricane is shown in Fig. 3.

The microgrid investigation for every hurricane-caused power outage includes three scenarios utilizing three different configurations of solar PV plant and fixed battery energy storage system (BESS) and Mobile battery energy storage system (BESS). Table 1 contains the configurations of the solar PV plant, fixed BESS, and Mobile BESS for the three scenarios of every power outage. For the BESS operations, the maximum and minimum state of charge (SOC) for BESS is set to 90% and 10%, respectively. Traditionally, we get to know when any hurricane is arriving from the weather forecast; it is assumed that the fixed BESS and Mobile BESS are charged and the BESS SOC is 90% when the simulation starts. For Mobile BESS, it can provide its rated power of 25 kW for three hours continuously. It is assumed that after providing power for 3 hours, the Mobile BESS will travel to the nearest charging station. Mobile BESS will be fully charged and return to supply power to

Table 1: Configuration of Three Scenarios for Every Hurricanes

Scenario	PV Size	Fixed BESS Size (kW)	Fixed BESS capacity(kWh)	Mobile BESS Size (kW)	Mobile BESS capacity(kWh)
1	50kW	50kW	100kWh	25kW	75kWh
2	150kW	150kW	300kWh	25kW	75kWh
3	250kW	250kW	500kWh	25kW	75kWh

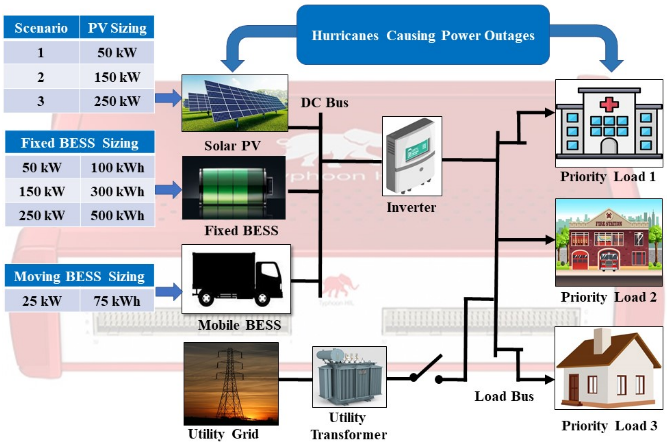

Figure 1: Overview of the UL-Cleco Microgrid Facility

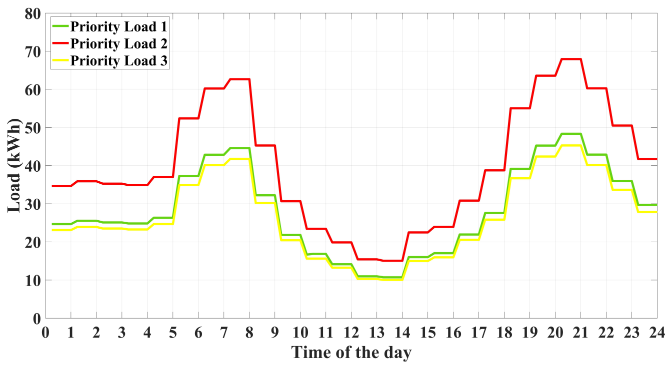

Figure 2: Different Priorities Load Data

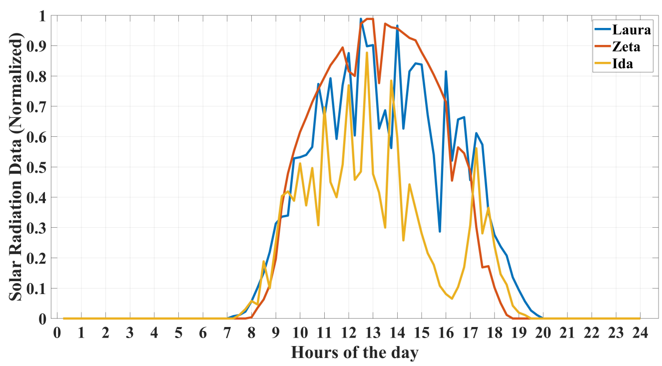

Figure 3: Solar Radiation Data (normalized) for Different Power Outages

this microgrid. This movement and charging time duration is considered to be 3 hours. Optimization of probable road congestion and shortest traveling path of the Mobile BESS is out of the scope of this paper. Typhoon HIL's real-time simulator is utilized to model and analyze the proposed microgrid control algorithm to study the high-fidelity performance of the microgrid in real-time.

3. Methodology

3.1. Proposed Resilience Metric

It requires a few hours to a few days to fully restore the power grid from power outages caused by natural disasters. Microgrids can be used to enhance resilience by supplying power during power outages. It is unrealistic to fulfill all the power demands when the main power grid suffers from a power outage. Hence, the loads can be classified based on their urgency. Considering 24-hour power outages caused by natural disasters, the amount of critical load served can be identified and investigated to determine the resilience level of the microgrid. Our proposed resilience metrics measure resilience value based on the amount of energy supplied to the load, focusing on the most critical loads. In recent literature [37; 38; 39; 40; 41; 42], researchers have placed five times more emphasis on the most critical loads than the least critical loads. The weighted factors of 5, 2.5, and 1 are assigned for priority load 1, priority load 2, and priority load 3, respectively. Thus, our proposed resilience metrics can be calculated utilizing the following equation.

$$Resilience, R = 5\beta_1 + 2.5\beta_2 + \beta_3 \tag{1}$$

Where,

$$\beta_1 = \frac{Served_{Load1}}{Demand_{Load1}} \tag{2}$$

$$\beta_2 = \frac{Served_{Load2}}{Demand_{Load2}} \tag{3}$$

$$\beta_3 = \frac{Served_{Load3}}{Demand_{Load3}} \tag{4}$$

In Eqn. (1), β_1 represents the ratio between the amount of served most critical load (kWh) and the total demand of the most critical load (kWh). Similarly, β_2 represents the ratio between the amount of served moderate critical load(kWh) and the total demand of the moderate critical load (kWh), β_3 represents the ratio between the amount of served least critical load (kWh) and the total demand of the least critical load (kWh). The maximum value of β_1, β_2, and β_3 can be 1 (if the total demands are fulfilled for the whole time duration), so 8.5

can be the maximum resilience value in our proposed resilience metrics. Utilizing our proposed resilience metrics, a single resilience value of a microgrid can be determined for the whole power outage duration(considering the highest importance of the demand satisfaction on the most critical load).

3.2. Technical Analysis

Our proposed microgrid control strategy is presented in Algorithm 1 - Resource Dispatch Algorithm. This microgrid control algorithm is crafted to fulfill the load demands during a power outage, putting maximum concentration on the most critical load satisfaction. This microgrid case study consists of a solar PV plant, fixed battery energy storage system (BESS), and Mobile BESS to supply the loads.

During the power outage, the proposed control system will coordinate the solar PV plant, fixed BESS, and Mobile BESS to supply the critical loads effectively for longer duration of hours. If the solar radiation stays at a higher amount for a longer time period and the availability of Mobile BESS, it looks to be a more efficient approach to charge the battery of fixed BESS to a certain level at first instead of satisfying the less critical load so that the microgrid achieves the capability to fulfill the priority load 1 for the greater amount of power outage hours. The proposed control system will continuously monitor the solar PV generation, battery state of charge (SOC), and load demands and will take necessary actions accordingly. When there is any solar PV generation, the control system will check the fixed battery SOC conditions and the availability of Mobile BESS to satisfy the load demands based on the fixed battery's SOC. If the fixed BESS SOC is greater than 70%, solar PV, fixed BESS, and Mobile BESS will fulfill all the load demands. If Mobile BESS is available, and the total load demand is higher than 25 kW, the solar PV, Mobile BESS, and the fixed BESS will supply the load demands together. If Mobile BESS is available, and the total load demand is less than 25 kW, the Mobile BESS will supply the loads, and the fixed BESS will go into charging mode. When the Mobile BESS is unavailable, if solar PV generation is higher than all the load demands, solar PV will satisfy the power demands by itself, and the extra generated PV power will go to the fixed BESS for its charging. If the solar-generated power is less than the power demands of all the loads, solar PV and fixed BESS will satisfy the load demands together.

When the fixed BESS SOC stays in the range between 70% to 40%, only priority loads 1 and 2 will be served, and priority load 3 will be curtailed. If Mobile BESS is available, and the combined demand for priority load 1 and priority load 2 is higher than 25 kW, the solar PV, Mobile BESS, and the fixed BESS will supply the load demands together. If Mobile BESS is available, and the load demand is less than 25 kW, the Mobile BESS will supply the loads, and the fixed BESS will go into charging mode. When the Mobile BESS is unavailable, if solar PV generation is higher than the combined demand for priority load 1 and priority load 2, solar PV will satisfy the power demands by itself, and the extra generated PV power will go to the fixed BESS for its charging. If the solar-generated power is less than the power demands of the combined demand for priority load 1 and priority load 2, solar PV and fixed BESS will satisfy the load demands together.

When the fixed BESS SOC stays in the range between 40% to 10%, only priority loads 1 will be served, and priority loads 2 & 3 will be curtailed. If Mobile BESS is available, and the combined demand for priority load 1 is higher than 25 kW, the solar PV, Mobile BESS, and the fixed BESS will supply the load demands together. If Mobile BESS is available, and the load demand is less than 25 kW, the Mobile BESS will supply the loads, and the fixed BESS will go into charging mode. When the Mobile BESS is unavailable, if solar PV generation is higher than the combined demand for priority load 1, solar PV will satisfy the power demands by itself, and the extra generated PV power will go to the fixed BESS for its charging. If the solar-generated power is less than the power demands of the combined demand for priority load 1, solar PV and fixed BESS will satisfy the load demands together.

When there is no solar PV generation, the fixed BESS and Mobile BESS will satisfy the loads. If the fixed BESS SOC remains higher than 80%, fixed BESS and Mobile BESS will fulfill all the load demands. If Mobile BESS is available, and the total load demand is higher than 25 kW, Mobile BESS and the fixed BESS will supply the load demands together. If Mobile BESS is available, and the total load demand is less than 25 kW, the Mobile BESS will supply the loads, and the fixed BESS will go into charging mode. When the Mobile BESS is unavailable, the fixed BESS will satisfy the load demands. When the fixed BESS SOC stays in the range between 80% to 50%, only priority loads 1 and 2 will be served, and priority load 3 will be curtailed. If Mobile BESS is available, and the combined demand for priority load 1 and priority load 2 is higher than 25 kW, the Mobile BESS and the fixed BESS will supply the load demands together. If Mobile BESS is available, and the load demand is less than 25 kW, the Mobile BESS will supply the loads, and the fixed BESS will go into charging mode. When the Mobile BESS is unavailable, the fixed BESS will satisfy the load demands of priority load 1 and priority load 2. When the fixed BESS SOC stays in the range between 50% to 10%, only priority loads 1 will be served, and priority loads 2 & 3 will be curtailed. If Mobile BESS is available, and the demand for priority load 1 is higher than 25 kW, the Mobile BESS and the fixed BESS will supply the load demands together. If Mobile BESS is available, and the load demand is less than 25 kW, the Mobile BESS will supply the loads, and the fixed BESS will go into charging mode. When the Mobile BESS is unavailable, the fixed BESS will satisfy the load demands of priority load 1.

3.3. Economic Analysis

This section also includes an economic analysis from different perspectives on economic indicators. For solar PV panels, 25 years is considered the average life duration [43; 44; 45]. This study considered a 24-year time horizon for the economic analysis of this microgrid study[46]. The time duration of solar PV inverter and BESS is 12 years and 10 years, respectively[47; 48]. In this analysis, 8 years is selected as the time duration of the solar PV inverter and BESS as the advanced features (i.e., Volt-VAR control, Volt-Watt control, etc.) shorten

Algorithm 1 Resource Dispatch Algorithm

```
Start
if PV > 0 then
    if Fixed BESS SOC ≥ 70% then
        if Mobile BESS is available: then
            if Load demand ≥ 25 kW then
                Supply all loads using Mobile BESS and Fixed BESS
            else
                Supply using Mobile BESS only, and charge Fixed BESS
            end if
        else
            Supply all loads using Fixed BESS
        end if
        Fixed BESS charges until SOC reaches 90%
    else if Fixed BESS SOC is between 40% and 70% then
        if Mobile BESS is available then
            if Load demand ≥ 25 kW then
                Supply only Priority Load 1 and Priority Load 2 using Mobile BESS and Fixed BESS
            else
                Supply using Mobile BESS only,and charge Fixed BESS
            end if
        else
            Supply only Priority Load 1 and Priority Load 2 using Fixed BESS
        end if
        Fixed BESS charges
    else if Fixed BESS SOC is between 10% and 40% then
        if Mobile BESS is available then
            if Load demand ≥25 kW then
                Supply only Priority Load 1 using Mobile BESS and Fixed BESS
            else
                Supply using Mobile BESS only, and charge Fixed BESS
            end if
        else
            Supply only Priority 1 loads using Fixed BESS
        end if
        Fixed BESS charges
    else
        if Mobile BESS is available then
            if Load demand ≥ 25 kW then
                Curtail all load and charge Fixed BESS
            else
                Supply Priority Load 1 using Mobile BESS only, and charge Fixed BESS
            end if
        else
            Curtail all load
        end if
        Fixed BESS will go on charging
    end if
else
    if Fixed BESS SOC is greater than or equal to 80% then
        if Mobile BESS is available then
            if Load demand ≥25 kW then
                Supply all loads using Mobile BESS and Fixed BESS
            else
                Supply using Mobile BESS only, and charge Fixed BESS
            end if
        else
            Supply all loads using Fixed BESS
        end if
    else if Fixed BESS SOC is between 50% and 80% then
        if Mobile BESS is available then
            if Load demand ≥25 kW then
                Supply Priority Load 1 and Priority Load 2 using Mobile BESS and Fixed BESS
            else
                Supply Priority Load 1 and Priority Load 2 using Mobile BESS only, and charge Fixed BESS
            end if
        else
            Supply Priority Load 1 and Priority Load 2 using Fixed BESS
        end if
    else if Fixed BESS SOC is between 10% and 50% then
        if Mobile BESS is available then
            if Load demand ≥25 kW then
                Supply Priority Load 1 using Mobile BESS and Fixed BESS
            else
                Supply Priority Load 1 using Mobile BESS only, and charge Fixed BESS
            end if
        else
            Supply Priority Load 1 using Fixed BESS
        end if
    else
        if Mobile BESS is available then
            if Load demand ≥25 kW then
                Curtail all loads
            else
                Supply Priority Load 1 using Mobile BESS only, and charge Fixed BESS
            end if
        else
            Curtail all loads
        end if
    end if
end if
End
```

the inverter's conventional lifetime [49]. Economic analyses are presented for all three hurricane scenarios. Furthermore, the investigation is extended to analyze the impact of the increased number of Hurricanes in a 24-year time horizon (considering 3 hurricanes in 1 set).

The revenue is generated from selling solar plus storage power to priority loads 1, 2, and 3. Using 5, the revenue, R can be found where E_i represents the energy supplied to the priority loads in kWh, and α is the selling price of solar plus storage energy in \$/kWh. Inflation factor, d is considered as 2.5% for this investigation [47]. During the power outages emergency supply, the value of α is considered as \$10/kWh, \$5/kWh, and \$2/kWh for priority load 1 (most critical load), priority load 2 (moderate critical load), and priority load 3 (least critical load), respectively [38; 39; 40; 41; 42]. For all the remaining regular days, the value of α is considered as \$0.10/kWh in this analysis.

$$R = \sum_{i=1}^{n} E_i \cdot \alpha \cdot (1+d)^{i-1} \tag{5}$$

Equation 6 calculates the cost of the solar PV system which is the algebraic summation of the market price of the solar PV panel, C_{PV}^{MAR}, operation and maintenance cost of the solar, C_{PV}^{OM}, and salvage value of the solar PV, C_{PV}^{SAL} [46]. Equation 7 calculates the cost of the solar PV inverter, which is the algebraic summation of the market price of the inverter, C_{INV}^{MAR}, operation and maintenance cost of the inverter, C_{INV}^{OM}, salvage value of the solar inverter, C_{INV}^{SAL} [46]. Equation 8 is used to compute total inverter expenditure for 24 year time period where S_{INV} is the rating of the inverter in kVA, d is the inflation factor, and T_R^{INV} is the lifetime of the inverter.

$$C_{PV} = C_{PV}^{MAR} + C_{PV}^{OM} - C_{PV}^{SAL} \tag{6}$$

$$\beta = C_{PV,INV}^{MAR} + C_{PV,INV}^{OM} - C_{PV,INV}^{SAL} \tag{7}$$

$$C_{PV,INV} = \sum_{j=1}^{n} S_{INV} \cdot \beta \cdot (1+d)^{(\frac{T_R^{INV}}{2})(j-1)} \tag{8}$$

The BESS expenditure is calculated based on its power and energy ratings using equation 9 and 10, respectively. Equation 9 is used to determine the BESS cost for power rating, γ, which is the algebraic summation of the market price of BESS for power rating, $C_{BESS,P}^{MAR}$, O&M cost of the BESS for power rating,$C_{BESS,P}^{OM}$, and the salvage value of BESS for power rating, $C_{BESS,P}^{SAL}$. Equations 10 is used to calculate the BESS cost for energy rating, η, and this calculation follows the same approach of the equation 9. η is determined using the market price of BESS for energy rating, $C_{BESS,E}^{MAR}$, O&M cost of the BESS for energy rating,$C_{BESS,E}^{OM}$, and the salvage value of BESS for energy rating, $C_{BESS,E}^{SAL}$. In equation 11, BESS cost for 24 years is calculated where the BESS lifetime, T_R^{BESS}, is considered as 8 years, and p is the BESS depreciation rate for each year, 2%. P_{BESS}, and E_{BESS} represent the power capacity and energy capacity of the battery, respectively. To calculate the battery inverter cost, equation 12 is utilized where the cost of the BESS inverter is the algebraic summation of the market price of the BESS inverter, $C_{BESS,INV}^{MAR}$, operation and maintenance cost of the BESS inverter, $C_{BESS,INV}^{OM}$, salvage value of the BESS inverter, $C_{BESS,INV}^{SAL}$. Compared to fixed BESS, Mobile BESS will likely add a cost premium of 5-10% associated with labor costs and transportation fuel costs [50]. For this case study, Mobile BESS cost is considered 7.5% higher than the fixed BESS.

$$\gamma = C_{BESS,P}^{MAR} + C_{BESS,P}^{OM} - C_{BESS,P}^{SAL} \tag{9}$$

$$\eta = C_{BESS,E}^{MAR} + C_{BESS,E}^{OM} - C_{BESS,E}^{SAL} \tag{10}$$

$$C_{BESS} = \sum_{k=1}^{n} [\gamma \cdot P_{BESS} + \eta \cdot E_{BESS}] \cdot (1-p)^{(T_R^{BESS}-1)(k-1)} \tag{11}$$

$$\delta = C_{BESS,INV}^{MAR} + C_{BESS,INV}^{OM} - C_{BESS,INV}^{SAL} \tag{12}$$

$$C_{BESS,INV} = \sum_{j=1}^{n} S_{BESS,INV} \cdot \delta \cdot (1+d)^{(\frac{T_R^{INV}}{2})(j-1)} \tag{13}$$

In table 2, all the input parameters of economic analysis and their corresponding values are included. Here, we included some economic indicators that measure the benefit of solar plus storage systems in power distribution systems for 24 years operation horizon [46].

- **Total cost**: the Total cost, C, is the summation of costs for solar PV panel, solar PV inverter, BESS, and BESS inverter expressed in 14[46].

$$C = C_{PV} + C_{PV,INV} + C_{BESS} + C_{BESS,INV} \tag{14}$$

- **Gained profit by solar system's owner**: The profit, P is the difference between the revenue and the total cost calculated using the equation 15. The revenue, R, expressed in the equation 5[46].

$$P = R - C. \tag{15}$$

- **Net Profit Margin**: The net profit margin NPM, or simply net margin, represents how much net income or profit is generated as a percentage of revenue made by solar system owner. The ratio represents the net profit to revenue for the owner of a solar system facility [46].

$$NPM = \frac{P}{R} \tag{16}$$

- **Net Present Value**: Two terms characterize the net present value (NPV), the present discounted value of costs PDC in (18) and the present discounted value of revenues PDR in (17) by $NPV = PDR - PDC$. Let's consider R_i to be the (undiscounted) revenues (benefits) of the solar system project during the year i and we consider C_i to be the (undiscounted) costs of the solar system project during the year i, afterward. We can calculate NPV using equation

(19). When the NPV is more than zero, the investment plan is considered profitable from the investor side [46].

$$PDR = \sum_{i=1}^{T} \frac{R_i}{(1+d)^{i-1}} \tag{17}$$

$$PDC = \sum_{i=1}^{T} \frac{C_i}{(1+d)^{i-1}} \tag{18}$$

$$NPV = \sum_{i=1}^{T} \frac{(R_i - C_i)}{(1+d)^{i-1}} \tag{19}$$

- **Revenue-Cost Ratio**: The revenue-cost ratio is the ratio of PDR to PDC which is mentioned in (20). When the RCR is greater than one, the investment plan will make revenue for the investor [46].

$$RCR = \frac{PDR}{PDC} = \frac{\sum_{i=1}^{T} \frac{R_i}{(1+d)^{i-1}}}{\sum_{i=1}^{T} \frac{C_i}{(1+d)^{i-1}}} \tag{20}$$

Table 2: Different Input Parameters of Economic Analysis

Parameters	Value	Reference
α	10, 5, 2, 0.1 (\$/kWh)	[38; 39; 40; 41; 42]
d	2.5%	[47]
C_{PV}^{MAR}	400 (\$/kW)	[47]
C_{PV}^{OM}	1% (\$/kW)	[51]
C_{PV}^{SAL}	10% (\$/kW)	[52]
C_{INV}^{MAR}	60 (\$/kW)	[47]
C_{INV}^{OM}	1% (\$/kW)	
C_{INV}^{SAL}	10% (\$/kW)	[52]
$C_{BESS,INV}^{MAR}$	50 (\$/kW)	[47]
$C_{BESS,INV}^{OM}$	1% (\$/kW)	
$C_{BESS,INV}^{SAL}$	10% (\$/kW)	[52]
$C_{BESS,P}^{MAR}$	628 (\$/kW)	[47]
$C_{BESS,P}^{OM}$	10 (\$/kW)	[48]
$C_{BESS,P}^{SAL}$	10% (\$/kW)	[52]
$C_{BESS,E}^{MAR}$	157 (\$/kWh)	[47]
$C_{BESS,E}^{OM}$	0.003 (\$/kW)	[48]
$C_{BESS,E}^{SAL}$	10% (\$/kW)	[52]
E_{BESS}	75, 100, 300, 500 (kWh)	
P_{BESS}	25, 50, 150, 250 (kW)	
p	2%	
S_{INV}	55, 162, 275 kVA	
T_R^{INV}	8 Years	
T_R^{BESS}	8 Years	

4. Results and Discussion

4.1. Technical Analysis

In this portion, the served amount of different categorized loads for all three scenarios of power outages will be presented and analyzed. In Fig. 4, the served load of Priority Loads 1, 2, and 3 are depicted for all three scenarios of the power outages caused by Hurricane Laura. For priority load 1, 52.48% of loads are served in scenario 1, whereas 85.15% loads are served in scenario 2. In scenario 3, all the 100% of priority load 1 is served successfully during the whole 24-hour power outage. For priority load 2, 18.97% loads are served in scenario 1, whereas 40.98% loads are served in scenario 2. In scenario 3, 53.64% of priority load 2 is served, which is the maximum amount for all three scenarios. For priority load 3, 7.51%, 22.45%, and 30.67% of loads are served in scenarios 1, 2, and 3, respectively. During all three scenarios, there is a tendency to increase served load for all the priority loads. Although around 30% priority load 1 is more served in scenario 2 than scenario 1, scenario 3 still shows the best performance by satisfying 100% priority load 1, which is the most critical load.

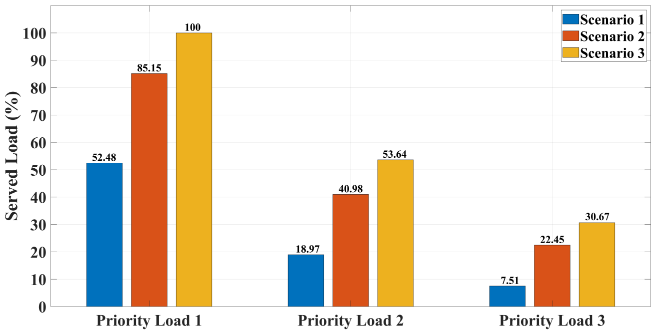

Figure 4: Served Loads for the Hurricane Laura (In Percent)

In Fig. 5, the served load of Priority Loads 1, 2, and 3 are presented for all three scenarios of power outages due to Hurricane Zeta. For priority load 1, 47.73% loads are satisfied in scenario 1, whereas 82.78% loads are satisfied in scenario 2. In scenario 3, 100% of priority load 1 is served successfully during the 24-hour power outage. For priority load 2, 19.18% loads are satisfied in scenario 1, whereas 36.61% loads are served in scenario 2. In scenario 3, 48.50% of priority load 2 is served. For priority load 3, 9.34%, 19.18% and 25.09% of loads are satisfied in scenarios 1, 2, and 3, respectively. During all three scenarios, there is also a similar pattern of increasing served load for all the categorized loads, like Hurricane Laura.

In Fig. 6, the served load of Priority Loads 1, 2, and 3 are presented for all three scenarios of power outages caused by Hurricane Ida. For priority load 1, 47.73% loads are served in scenario 1, whereas 82.65% loads are served in scenario 2. In scenario 3, 100% of priority load 1 demand is served successfully during the whole 24 hours of power outage. For priority load 2, 11.65% loads are satisfied in scenario 1, whereas 37.05% loads are served in scenario 2. In scenario 3, 49.30% of priority load 2 is satisfied. For priority load 3, 5.85%, 11.05%,

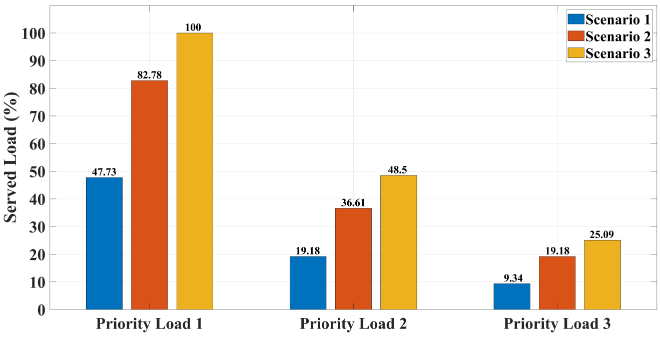

Figure 5: Served Loads for the Hurricane Zeta (In Percent)

and 26.86% of loads are served in scenarios 1, 2, and 3, respectively. During all three scenarios, there is a tendency to increase served load for all the priority loads. Most importantly, the amount of served loads of priority load 1 is almost doubled in scenario 2 compared to scenario 1, whereas scenario 3 shows the best performance by fulfilling 100% of the most critical load demand.

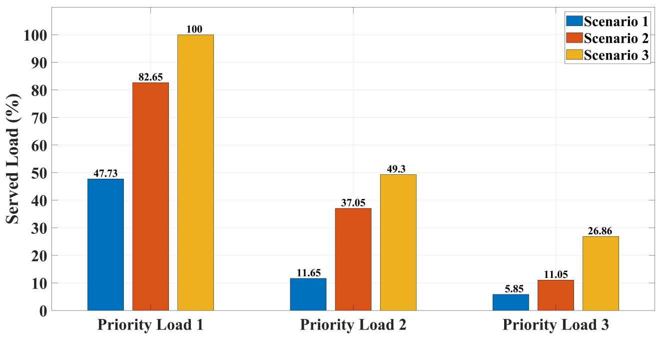

Figure 6: Served Loads for the Hurricane Ida (In Percent)

Our proposed microgrid control algorithm concentrates on satisfying the priority load 1 (most critical load) during 24 24-hour power outage. Fig. 7 presents the time duration of the most critical load serving. For Hurricane Laura, the most critical load is satisfied for 65.63% hours of the 24 hours in scenario 1, whereas the most critical load is served in scenario 2 for 88.54% hours of the 24 hours. Scenario 3 shows the best performance by satisfying 100% of the most critical load for 24 hours. For Hurricane Zeta, the most critical load is satisfied for 62.5% hours of the 24 hours in scenario 1, whereas the most critical load is served in scenario 2 for 86.46% hours of the 24 hours. Scenario 3 shows the best performance among all three scenarios by satisfying the most critical load for 100% hours of the whole 24 hours. For Hurricane Ida, the most critical load is satisfied for 62.5% hours of the 24 hours in scenario 1, whereas the most critical load is served in scenario 2 for 87.5% hours of the 24 hours. Scenario 3 shows the best performance among all three scenarios by fulfilling 100% of the most critical load for the whole 24 hours.

In Fig. 8, Fig. 9, Fig. 10, battery SOC profiles for all the scenarios of the power outages are presented. In Fig. 8, the battery SOC for all three scenarios is provided for Hurricane

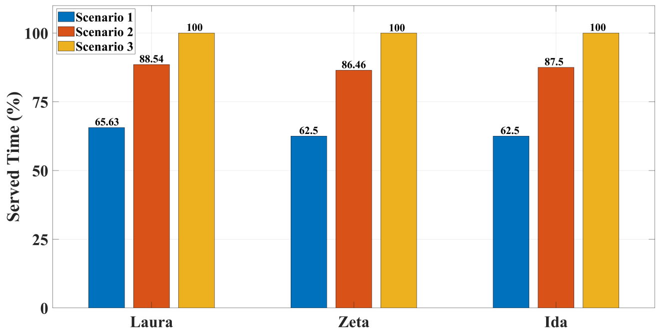

Figure 7: Serving Time Duration of Most Critical Load (In Percent)

Laura. In scenario 1, the battery SOC stays at 10% for around 7 hours, which is the highest duration of hours in all the scenarios. 10% SOC indicates that no loads are served during that time horizon. In scenario 2, the battery SOC shows better characteristics, and SOC stays at 10% for around 2 hours. The SOC stays at 90% for around 5.5 hours, indicating that all the loads are served during that time. In scenario 3, the minimum SOC never goes below 20%, indicating that at least priority load 1 is served for 24 hours. The SOC remains 90% for around 7 hours, indicating that all the loads are served during that time.

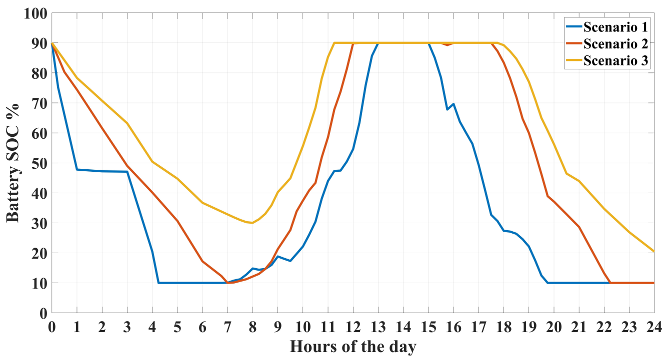

Figure 8: Battery SOC for the Hurricane Laura

In Fig. 9, the battery SOC for all three scenarios of the power outage caused by Hurricane Zeta. In scenario 1, the battery SOC stays at 10% for around 8 hours, which is the highest duration of hours in all the scenarios. In scenario 2, the battery SOC shows better characteristics, and SOC stays at 10% for around 2.5 hours. The SOC stays at 90% for around 5.5 hours, indicating that all the loads are served during that time. In scenario 3, the minimum SOC never goes below 17%, indicating that at least priority load 1 is served for 24 hours. The SOC remains 90% for around 6 hours, indicating that all the loads are served during that time.

In Fig. 10, the battery SOC for all three scenarios of the power outage caused by Hurricane Zeta. In scenario 1, the battery SOC stays at 10% for around 8 hours, which is the highest duration of hours in all the scenarios. In scenario 2, the battery SOC shows better characteristics, and SOC stays at 10% for around 2 hours. The SOC stays at 90% for around 2.5 hours, indicating that all the loads are served during that time. In sce-

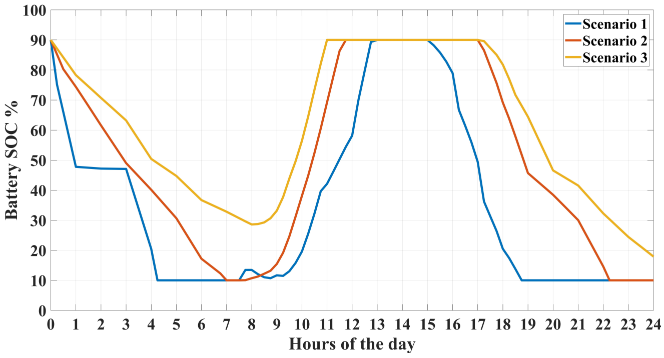

Figure 9: Battery SOC for the Hurricane Zeta

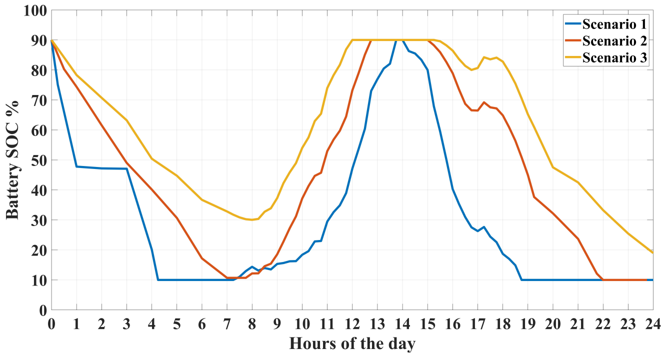

Figure 10: Battery SOC for the Hurricane Ida

nario 3, the minimum SOC never goes below 18%, which indicates that at least priority load 1 is served for the whole 24 hours. The SOC remains 90% for around 3.5 hours, indicating that all the loads are served during that time.

4.2. Resilience Value

After completing the simulation for all three scenarios of power outages caused by Hurricane Laura, Zeta, and Ida and determining the amount of served load for each scenario of the power outages, resilience values have been calculated using the equations of 1, 2, 3, 4. All the resilience values are presented in Table 3.

Table 3: Resilience Value for Different Power Outages

Hurricanes	Scenarios	Resilience Value, R
Laura	1	3.17
	2	5.50
	3	6.64
Zeta	1	2.95
	2	5.24
	3	6.46
Ida	1	2.73
	2	5.16
	3	6.50

Resilience values of scenarios 1, 2, and 3 for the power outages caused by Hurricane Laura are 3.17, 5.50, and 6.64, respectively. Resilience values of scenarios 1, 2, and 3 for the power outages caused by Hurricane Zetaa are 2.95, 5.24, and 6.46, respectively. The resilience values of scenarios 1, 2, and 3 for the power outages caused by Hurricane Ida are 2.73, 5.16, and 6.50, respectively.

4.3. Economic Analysis

Table 4 shows the investment required for 24 years, considering different microgrid configuration scenarios 1, 2, and 3, respectively. Scenario 1 requires 216.97 thousand US dollars, whereas Scenario 2 requires 512.88 thousand dollars, which is more than 2.3 times the investment of Scenario 1. Scenario 3 requires the maximum investment among all three scenarios, 808.78 thousand dollars.

Table 4: Investment for Three Scenarios (in thousands US $)

	Scenario 1	Scenario 2	Scenario 3
Investment	216.97	512.88	808.78

Table 5 depicts the profit generated during 24 years time duration of microgrid operation for all three configuration scenarios considering different numbers of hurricane sets. For one hurricane set (considering 3 hurricanes in 1 set) in 24 years, the profit of scenarios 1, 2, and 3 is 406.00, 832.10, and 911.90 thousand US dollars, respectively. For five hurricane sets (considering 3 hurricanes in 1 set) in 24 years, the profit of scenarios 1, 2, and 3 is 471.50, 952.90, and 1061.50 thousand US dollars, respectively. It is visible that the financial profit is increasing with the increasing number of hurricane sets for all three scenarios, and scenario 3 is the leading profit generator among all the hurricane sets.

Table 5: Profit for Three Scenarios of Different Hurricane Sets (in thousands $)

Hurricane Sets	Scenario 1	Scenario 2	Scenario 3
1	406.00	832.10	911.90
2	419.60	857.20	943.00
3	434.90	885.40	977.90
4	452.20	917.20	1017.30
5	471.50	952.90	1061.50

In order to investigate the impacts of different numbers of hurricane sets in all three scenarios, NPV, NPM, and RCR, are utilized for all three scenarios considering the number of hurricane sets from 1 to 5. In Fig. 11, NPV is increasing for all three scenarios with the increasing number of hurricane sets. Among all the hurricane sets, scenario 1 has the lowest NPV in all three scenarios. Although scenario 2 has the highest NPV for all the hurricane sets, scenario 3 is approaching to merge on scenario 2 with the increased number of hurricane sets. In Fig. 12, NPM curves depicts the net profit margin for different hurricane sets.

For all the different hurricane sets, NPM gradually increases for all three scenarios. Furthermore, scenario 1 leads to scenarios 2 and 3 for all the hurricane sets. In Fig. 13, RCR graphs are presented for all three scenarios of different numbers of hurricane sets. For all the hurricane sets, all three scenarios have RCR value greater than 1, and the RCR value increases with the increasing number of hurricane sets.

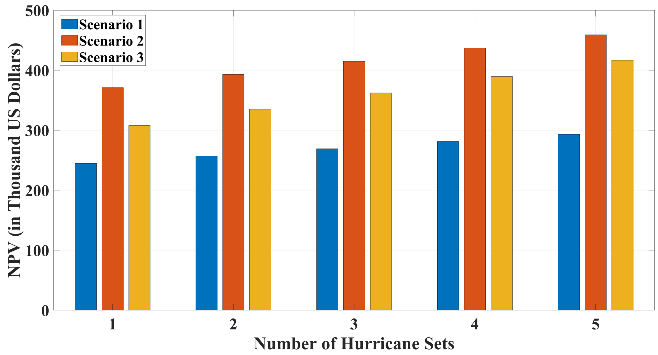

Figure 11: Net Present Value (NPV)

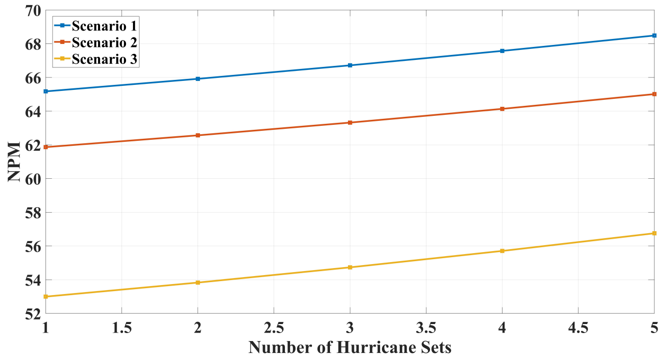

Figure 12: Net Profit Margin (NPM)

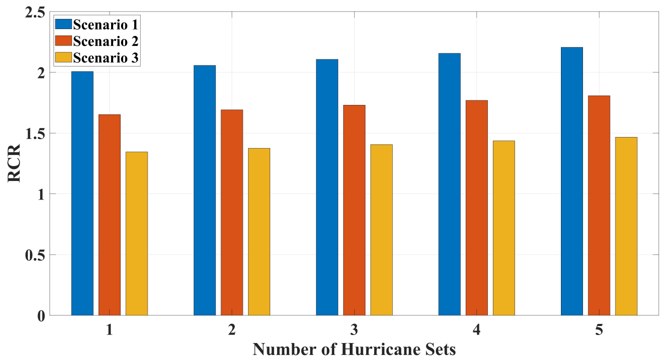

Figure 13: Revenue-Cost Ratio (RCR)

The resilience values of scenarios 1, 2, and 3 for every power outages caused by Hurricanes Laura, Zeta, and Ida are taken from Table 3 and the investment required for scenarios 1, 2, and 3 from Table 4 are utilized to present the resilience vs investment curve in Fig. 14. In Fig. 14, it can be observed that after increasing investment from 216.97 thousand US dollars to 512.88 thousand US dollars, resilience value increased sharply for all the outages. When the investment increased from 512.88 thousand US dollars to 808.78 thousand US dollars, resilience value followed an increasing tendency with the increase of investment, reaching the highest resilience level.

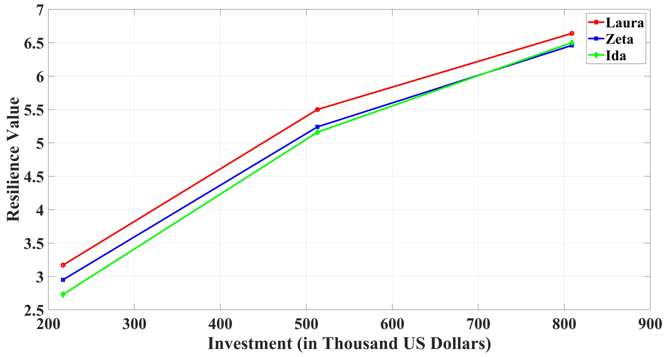

Figure 14: Resilience vs Investment Curve

5. Summary and conclusions

In conclusion, our research has demonstrated the significant potential of integrating both stationary and mobile battery storage systems (BSS) within microgrids to enhance energy resilience, particularly in the face of natural disasters. The study's findings reveal that strategic deployment and real-time operation of these systems can substantially reduce unserved loads, ensuring the continuous provision of power to critical infrastructure. Moreover, our economic analysis underscores the financial viability of such investments, highlighting that with careful planning and implementation, microgrids can offer a cost-effective solution to improve resilience. The insights gained from this research provide a valuable framework for decision-makers in the energy sector, suggesting that the integration of stationary and mobile BSS within microgrids is a promising avenue for enhancing energy resilience in disaster-prone areas.

Acknowledgements

This research work is partially supported by the Louisiana Board of Regents, ITRS program as well as Cleco Power under the grant# LEQSF(2022-25)-RD-B-05

References

[1] S. Yankson, S. S. Ullah, S. Ebrahimi, F. Ferdowsi, K. A. Ritter, and T. Chambers, "Resilience-enabling load flexibility and resource adequacy investment in microgrids," in *2023 IEEE Texas Power and Energy Conference (TPEC)*. IEEE, 2023, pp. 1–6.

[2] M. A. Igder, X. Liang, and M. Mitolo, "Service restoration through microgrid formation in distribution networks: A review," *IEEE Access*, vol. 10, pp. 46 618–46 632, 2022.

[3] M. E. Khodayar, M. Barati, and M. Shahidehpour, "Integration of high reliability distribution system in microgrid operation," *IEEE Transactions on Smart Grid*, vol. 3, no. 4, pp. 1997–2006, 2012.

[4] Y. Lin, J. Wang, and M. Yue, "Equity-based grid resilience: How do we get there?" *The Electricity Journal*, vol. 35, no. 5, p. 107135, 2022.

[5] M. Hamidieh and M. Ghassemi, "Microgrids and resilience: A review," *IEEE Access*, 2022.

[6] N. Bhusal, M. Abdelmalak, M. Kamruzzaman, and M. Benidris, "Power system resilience: Current practices, challenges, and future directions," *Ieee Access*, vol. 8, pp. 18 064–18 086, 2020.

[7] E. Hossain, S. Roy, N. Mohammad, N. Nawar, and D. R. Dipta, "Metrics and enhancement strategies for grid resilience and reliability during natural disasters," *Applied energy*, vol. 290, p. 116709, 2021.

[8] T. Adefarati and R. Bansal, "Reliability and economic assessment of a microgrid power system with the integration of renewable energy resources," *Applied Energy*, vol. 206, pp. 911–933, 2017.

[9] G. Fu, S. Wilkinson, R. J. Dawson, H. J. Fowler, C. Kilsby, M. Panteli, and P. Mancarella, "Integrated approach to assess the resilience of future electricity infrastructure networks to climate hazards," *IEEE Systems Journal*, vol. 12, no. 4, pp. 3169–3180, 2017.

[10] C. Shao, M. Shahidehpour, X. Wang, X. Wang, and B. Wang, "Integrated planning of electricity and natural gas transportation systems for enhancing the power grid resilience," *IEEE Transactions on Power Systems*, vol. 32, no. 6, pp. 4418–4429, 2017.

[11] J. Dugan, D. Byles, and S. Mohagheghi, "Social vulnerability to long-duration power outages," *International Journal of Disaster Risk Reduction*, vol. 85, p. 103501, 2023.

[12] A. H. Rodríguez, A. Shafieezadeh, and A. Yilmaz, "How important are socioeconomic factors for hurricane performance of power systems? an analysis of disparities through machine learning," in *2022 IEEE International Conference on Power Systems Technology (POWERCON)*. IEEE, 2022, pp. 1–6.

[13] D. Mitsova, A.-M. Esnard, A. Sapat, and B. S. Lai, "Socioeconomic vulnerability and electric power restoration timelines in florida: the case of hurricane irma," *Natural Hazards*, vol. 94, pp. 689–709, 2018.

[14] S. Azad and M. Ghandehari, "A study on the association of socioeconomic and physical cofactors contributing to power restoration after hurricane maria," *IEEE Access*, vol. 9, pp. 98 654–98 664, 2021.

[15] M. P. Korukonda, S. Pandey, H. Zheng, A. Alabdulwahab, A. Abusorrah, and M. Shahidehpour, "A quantitative framework to evaluate the resilience enhancement in power distribution feeders during adverse weather events," in *2023 5th Global Power, Energy and Communication Conference (GPECOM)*. IEEE, 2023, pp. 425–430.

[16] A. F. Malek, H. Mokhlis, N. N. Mansor, J. J. Jamian, L. Wang, and M. A. Muhammad, "Power distribution system outage management using improved resilience metrics for smart grid applications," *Energies*, vol. 16, no. 9, p. 3953, 2023.

[17] M. Shadaei, A. Hosseinipour, and J. Khazaei, "Time-domain operational metrics for real-time resilience assessment in dc microgrids," *arXiv preprint arXiv:2312.03609*, 2023.

[18] S. N. Jahromi, E. Hajipour, and M. Ehsan, "Optimal resilience-oriented microgrid formation considering failure probability of distribution feeders," *Electric Power Systems Research*, vol. 209, p. 108012, 2022.

[19] O. Q. Simental, P. Mandal, and E. Galvan, "Enhancing distribution grid resilience to power outages using electric vehicles in residential microgrids," in *2021 North American Power Symposium (NAPS)*. IEEE, 2021, pp. 01–06.

[20] O. Q. Simental, P. Mandal, E. Galvan, and Z. Wang, "Leveraging distributed evs and pvs to assess networked microgrids resilience against extreme weather event," in *2022 IEEE Power & Energy Society General Meeting (PESGM)*. IEEE, 2022, pp. 1–5.

[21] J. Marqusee, W. Becker, and S. Ericson, "Resilience and economics of microgrids with pv, battery storage, and networked diesel generators," *Advances in Applied Energy*, vol. 3, p. 100049, 2021.

[22] D. Qiu, Y. Wang, T. Zhang, M. Sun, and G. Strbac, "Hierarchical multi-agent reinforcement learning for repair crews dispatch control towards multi-energy microgrid resilience," *Applied Energy*, vol. 336, p. 120826, 2023.

[23] S. Lei, J. Wang, C. Chen, and Y. Hou, "Mobile emergency generator pre-positioning and real-time allocation for resilient response to natural disasters," *IEEE Transactions on Smart Grid*, vol. 9, no. 3, pp. 2030–2041, 2016.

[24] H. Saboori, "Enhancing resilience and sustainability of distribution networks by emergency operation of a truck-mounted mobile battery energy storage fleet," *Sustainable Energy, Grids and Networks*, vol. 34, p. 101037, 2023.

[25] M.-H. Khooban, M. Gheisarnejad, N. Vafamand, M. Jafari, S. Mobayen, T. Dragicevic, and J. Boudjadar, "Robust frequency regulation in mobile microgrids: Hil implementation," *IEEE Systems Journal*, vol. 13, no. 4, pp. 4281–4291, 2019.

[26] J. Dugan, S. Mohagheghi, and B. Kroposki, "Application of mobile energy storage for enhancing power grid resilience: A review," *Energies*, vol. 14, no. 20, p. 6476, 2021.

[27] M. Knowledge, "Pg&e adds tesla mobile energy storage to island test in foothills microgrid," https://www.microgridknowledge.com/community-microgrids/article/33010171/pge-adds-tesla-mobile-energy-storage-to-island-test-foothills-microgrid, 2021.

[28] E. Karan, "Mobile emergency power during and after natural disasters and shortages," 2023.

[29] X. Guo, G. Miao, X. Wang, L. Yuan, H. Ma, and B. Wang, "Mobile energy storage system scheduling strategy for improving the resilience of distribution networks under ice disasters," *Processes*, vol. 11, no. 12, p. 3339, 2023.

[30] Q. Shi, H. Wan, W. Liu, H. Han, Z. Wang, and F. Li, "Preventive allocation and post-disaster cooperative dispatch of emergency mobile resources for improved distribution system resilience," *International Journal of Electrical Power & Energy Systems*, vol. 152, p. 109238, 2023.

[31] H. Wu, Y. Xie, Y. Xu, Q. Wu, C. Yu, and J. Sun, "Robust coordination of repair and dispatch resources for post-disaster service restoration of the distribution system," *International Journal of Electrical Power & Energy Systems*, vol. 136, p. 107611, 2022.

[32] M. Nazemi, P. Dehghanian, X. Lu, and C. Chen, "Uncertainty-aware deployment of mobile energy storage systems for distribution grid resilience," *IEEE Transactions on Smart Grid*, vol. 12, no. 4, pp. 3200–3214, 2021.

[33] A. K. Erenoğlu and O. Erdinç, "Real-time allocation of multi-mobile resources in integrated distribution and transportation systems for resilient electrical grid," *IEEE Transactions on Power Delivery*, vol. 38, no. 2, pp. 1108–1119, 2022.

[34] S. Yao, P. Wang, X. Liu, H. Zhang, and T. Zhao, "Rolling optimization of mobile energy storage fleets for resilient service restoration," *IEEE Transactions on Smart Grid*, vol. 11, no. 2, pp. 1030–1043, 2019.

[35] S. Lei, J. Wang, C. Chen, and Y. Hou, "Mobile emergency generator pre-positioning and real-time allocation for resilient response to natural disasters," *IEEE Transactions on Smart Grid*, vol. 9, no. 3, pp. 2030–2041, 2016.

[36] D. J. Veerendra Kumar, L. Deville, K. A. Ritter III, J. R. Raush, F. Ferdowsi, R. Gottumukkala, and T. L. Chambers, "Performance evaluation of 1.1 mw grid-connected solar photovoltaic power plant in louisiana," *Energies*, vol. 15, no. 9, p. 3420, 2022.

[37] H. Gao, Y. Chen, S. Mei, S. Huang, and Y. Xu, "Resilience-oriented pre-hurricane resource allocation in distribution systems considering electric buses," *Proceedings of the IEEE*, vol. 105, no. 7, pp. 1214–1233, 2017.

[38] S. Yao, T. Zhao, H. Zhang, P. Wang, and L. Goel, "Two-stage stochastic scheduling of transportable energy storage systems for resilient distribution systems," in *2018 IEEE International Conference on Probabilistic Methods Applied to Power Systems (PMAPS)*. IEEE, 2018, pp. 1–6.

[39] S. Yao, P. Wang, and T. Zhao, "Transportable energy storage for more resilient distribution systems with multiple microgrids," *IEEE Transactions on Smart Grid*, vol. 10, no. 3, pp. 3331–3341, 2018.

[40] S. Yao, P. Wang, X. Liu, H. Zhang, and T. Zhao, "Rolling optimization of mobile energy storage fleets for resilient service restoration," *IEEE Transactions on Smart Grid*, vol. 11, no. 2, pp. 1030–1043, 2019.

[41] S. Yao, J. Gu, H. Zhang, P. Wang, X. Liu, and T. Zhao, "Resilient load restoration in microgrids considering mobile energy storage fleets: A deep reinforcement learning approach," in *2020 IEEE Power & Energy Society General Meeting (PESGM)*. IEEE, 2020, pp. 1–5.

[42] M. Nazemi, P. Dehghanian, X. Lu, and C. Chen, "Uncertainty-aware deployment of mobile energy storage systems for distribution grid resilience," *IEEE Transactions on Smart Grid*, vol. 12, no. 4, pp. 3200–3214, 2021.

[43] K. Anusuya, K. Vijayakumar, and S. Manikandan, "From efficiency to eternity: A holistic review of photovoltaic panel degradation and end-of-life management," *Solar Energy*, vol. 265, p. 112135, 2023.

[44] M. S. Chowdhury, K. S. Rahman, T. Chowdhury, N. Nuthammachot,

K. Techato, M. Akhtaruzzaman, S. K. Tiong, K. Sopian, and N. Amin, "An overview of solar photovoltaic panels' end-of-life material recycling," *Energy Strategy Reviews*, vol. 27, p. 100431, 2020.

[45] V. Tan, P. R. Dias, N. Chang, and R. Deng, "Estimating the lifetime of solar photovoltaic modules in australia," *Sustainability*, vol. 14, no. 9, p. 5336, 2022.

[46] S. S. Ullah, S. Ebrahimi, F. Ferdowsi, and M. Barati, "Techno-economic impacts of volt-var control on the high penetration of solar pv interconnection," *Cleaner Energy Systems*, p. 100067, 2023.

[47] V. Ramasamy, J. Zuboy, E. O'Shaughnessy, D. Feldman, J. Desai, M. Woodhouse, P. Basore, and R. Margolis, "Us solar photovoltaic system and energy storage cost benchmarks, with minimum sustainable price analysis: Q1 2022," National Renewable Energy Lab.(NREL), Golden, CO (United States), Tech. Rep., 2022.

[48] K. Mongird, V. Viswanathan, P. Balducci, J. Alam, V. Fotedar, V. Koritarov, and B. Hadjerioua, "An evaluation of energy storage cost and performance characteristics," *Energies*, vol. 13, no. 13, p. 3307, 2020.

[49] O. Gandhi, C. D. Rodríguez-Gallegos, N. B. Y. Gorla, M. Bieri, T. Reindl, and D. Srinivasan, "Reactive power cost from pv inverters considering inverter lifetime assessment," *IEEE Transactions on Sustainable Energy*, vol. 10, no. 2, pp. 738–747, 2018.

[50] "Mobile Energy Storage Study: Emergency Response and Demand Reduction," Massachusetts Department of Energy Resource: Boston, MA, USA, Tech. Rep., 2020.

[51] L. Deotti, W. Guedes, B. Dias, and T. Soares, "Technical and economic analysis of battery storage for residential solar photovoltaic systems in the brazilian regulatory context," *Energies*, vol. 13, no. 24, p. 6517, 2020.

[52] K. Humphreys and D. Brown, "Life-cycle cost comparisons of advanced storage batteries and fuel cells for utility, stand-alone, and electric vehicle applications," Pacific Northwest Lab., Richland, WA (USA), Tech. Rep., 1990.